27 May 2010, 4:30 pm - 6:20 pm

Effect of Canyon Geometry and Ground Conditions on the Seismic Performance of Tendaho Earthfill Dam in Ethiopia.

Tensay G. Berhe
Institute of Geotechnical Engineering, BOKU, Austria

Wu Wei
Institute of Geotechnical Engineering, BOKU, Austria

Recommended Citation

Berhe, Tensay G. and Wei, Wu, "Effect of Canyon Geometry and Ground Conditions on the Seismic Performance of Tendaho Earthfill Dam in Ethiopia." (2010). *International Conferences on Recent Advances in Geotechnical Earthquake Engineering and Soil Dynamics*. 16.
https://scholarsmine.mst.edu/icrageesd/05icrageesd/session04b/16

Fifth International Conference on
Recent Advances in Geotechnical Earthquake Engineering and Soil Dynamics
and Symposium in Honor of Professor I.M. Idriss
May 24-29, 2010 • San Diego, California

EFFECT OF CANYON GEOMETRY AND GROUND CONDITIONS ON THE SEISMIC PERFORMANCE OF TENDAHO EARTHFILL DAM IN ETHIOPIA.

Tensay G. Berhe
Institute of Geotechnical Engineering, BOKU.
Vienna, A-1180, Feistmantel straße 4, Austria

Wei, Wu
Institute of Geotechnical Engineering, BOKU.
Vienna, A-1180, Feistmantel straße 4, Austria

ABSTRACT

The seismic performance of earth dams is usually studied by two dimensional (2D) space. However, considerable judgment is required to estimate the overall three dimensional dynamic response of dams in a narrow canyon from plane strain analyses of individual sections of the dam. This is so because the plane strain analysis normally ignores the arching effect of the valley which is particularly relevant for dams in narrow valleys. Because of the arching action, the effect of the canyon geometry on the dynamic response of earth dams will be a stiffening of the system. The effect of the canyon geometry is studied by carrying out 3D model of a dam site using a finite difference code, FLAC3D. The assumed 3D model contains all details of the dam body and foundation materials but with variable valley configuration of Tendaho earthfill dam. The mentioned dam is an earth fill dam located in the Afar regional state of Ethiopia. The area is a seismically active area as it lies on the East African Rift valley which can generate earthquake of magnitude greater than 6. In addition, the alluvium foundation of the dam consists of granular materials, which may liquefy during strong earthquakes. In this paper, the numerical results for the different 3D simulations are compared and correlated. Moreover, the seismic performance of the Tendaho earth fill dam is investigated. From the results of the analyses and correlations created, the canyon geometry under which three dimensional behavior is of importance in the dynamic response of a dam are determined. And the resulting correlation is then applied to the Tendaho earthfill dam.

INTRODUCTION

If a portion of an otherwise rigid support of granular soil mass yields, the particles adjoining the yielding part move cut of their original position between adjacent stationary granular mass. This relative movement within the granular masses is opposed by shearing resistance within the zone of contact between the yielding and stationary masses. Since the shearing resistance tends to keep the yielding mass in its original position, the pressure on the yielding part of the support is reduced and the pressure on the stationary parts is increased. This transfer of pressure from a yielding part to adjacent non-yielding parts of a soil mass is called the arching effect. Arching also occurs when one part of a support yields more than the adjacent parts. The same phenomenon prevails also in the deformation characteristics of embankments and earthfill dams especially when they are constructed in narrow valley. In numerical simulations, it is usually intended to simplify the real structure by eliminating regions that are believed to have minor impact on the desired results. This is mainly due to the lack of proper simulating tools, as well as insufficient knowledge of the relevant affecting factors. One of the important stages in the design of earth dams is the exact evaluation of irrecoverable volume and porewater pressure through out the dam body as a result of shaking. This can be explained in terms of evaluating the seismic performance of the dam.

The seismic performance of earthfill dams is often performed in two dimensional (2D) space, which demands selection of the critical cross sections of the dam. In other words the problem is treated as plane strain problem. However, considerable judgment is required to estimate the overall three dimensional dynamic response of a dam in a narrow canyon from plane strain analyses of individual critical sections of the dam. In addition as the two dimensional consideration requires such simplifications as eliminating the effect of the canyon geometry, the two dimensional deformation analysis is believed to render inaccurate results. This is so because the plane strain analysis normally ignores the arching effect of the valley which is particularly relevant for dams in narrow valleys. Because of the arching action, the effect of the canyon geometry on the dynamic response of earth dams will be a stiffening of the system. For this purpose the effect of the canyon geometry is studied by carrying out 3D model of a real dam site. The assumed 3D model contains all details of the dam body and its foundation of Tendaho earthfill dam in Ethiopia but with variable valley configuration.

Since the 1971 San Fernando earthquake in California (Ming and Li, 2003), major progress has been achieved in the understanding of the earthquake action on dams. Gazetas (1987) discussed the historical developments of theoretical methods for estimating the dynamic response of earth dams to earthquake ground excitation. He outlined their important features, their advantages and limitations. Progress in the area of geotechnical computation and numerical modeling offers interesting facilities for the analysis of the dam response in considering complex issues such as the soil non linearity, the evolution of the pore pressure during the dam construction procedure and real earthquake records. Detailed analysis techniques include equivalent linear (decoupled) solutions, and non linear finite element and finite difference coupled or decoupled formulations.

Tendaho dam project over river Awash is located in the north-east of Addis Ababa, capital city of Ethiopia. It is among the largest dams in the country. It is a zoned earthfill dam with fill volume of about 4 Mm^3 and expected to impound about 1.8 Bm^3 water for irrigation purpose. The length of the dam crest is about 412 m and its maximum height at the river section is about 53 m. The width of the dam is about 10 m at the crest and 412 m at the widest point in the foundation level. The Tendaho dam is built on an alluvium consisting of alternating layers of mudstones siltstones, conglomerates and sandstones.

GEOLOGICAL SETTING OF DAM SITE

Tendaho dam site is located within an area known as the Tendaho graben, which forms the center of Afar triangle. The volcanic rocks are composed of material of sea floor spreading as a result of crustal plate separation of Arabia and Africa during Tertiary times. The uplifted sea floor forms now a part of Tendaho graben. Due to tensile tectonic strain acting along three rift lineations, the NW–SE oriented Tendaho graben, a fault-bounded basin, is formed. Escarpment of Tendaho forms the south – western boundary of this basin. From early periods, lake development has infilled the Tendaho graben with various types of sedimentary deposits ranging from clay to gravel, volcanic tuffs, ash with limestone crusts and hot spring deposits.

In the river channel area and immediate banks recent alluvial deposits of silt and gravel overlie consolidated older sedimentary materials, which are thought to be lakebeds. These lake deposits have variable thickness and boreholes have proved it to be more than 50 m thick.

The cores from the boreholes show the lake deposit to be a mixed assemblage of silt, clay, sand, calcareous inclusions, mudstones, sand stones, and conglomerates. The typical geological profile of the dam site is shown in Fig. 1.

A preliminary investigation of the alluvium foundation materials and dam body indicates that they contain liquefiable granular materials that are susceptible for liquefaction. In particular the liquefaction susceptibility based on grain size distribution shows that over 90% of the alluvium foundation soils lie within the boundaries for potentially liquefiable soils as shown in Fig. 2.

The dam site is located in western and southern parts of highly complex fault zone of Afar triangle. Many of the fault scarps are of recent date and the area is seismically active. From the regional seismicity review, earthquakes with magnitude, M, greater than 6 can be expected. The Tendaho dam design project recommends a peak acceleration of 0.18g for the OBE. Moreover, the regional seismicity study required 0.3g for the MCE .

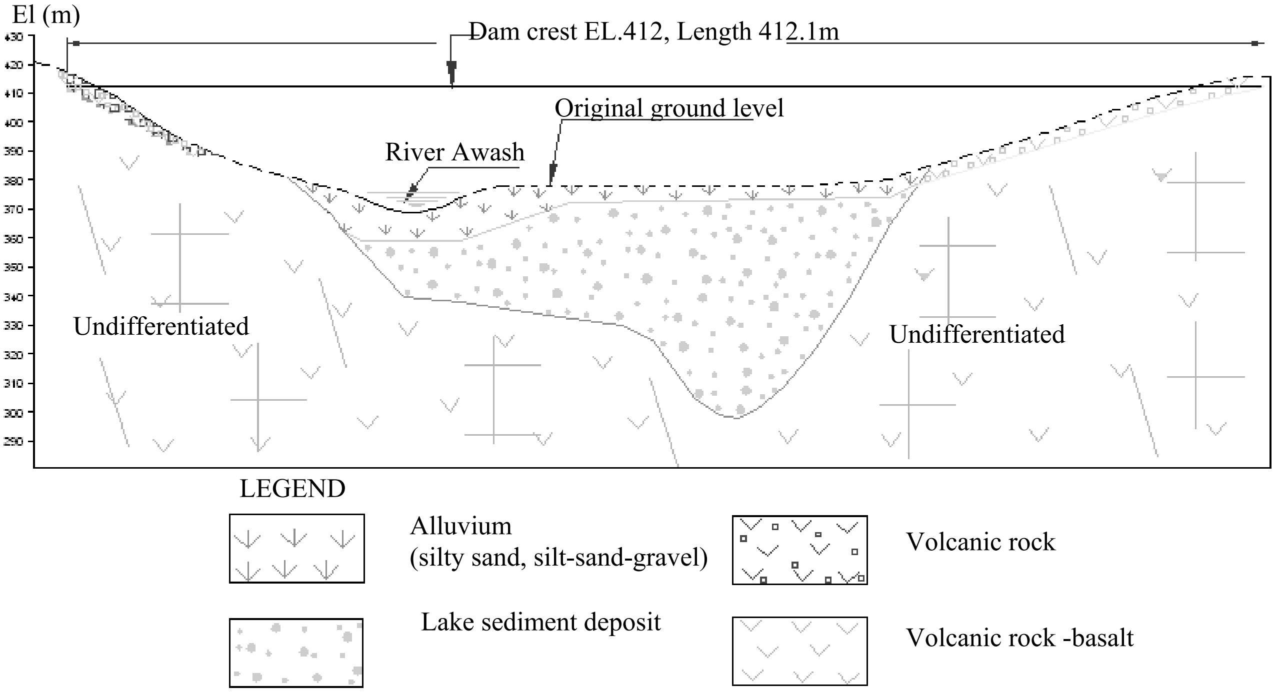

Fig. 1. Typical geological profile along the dam axis.

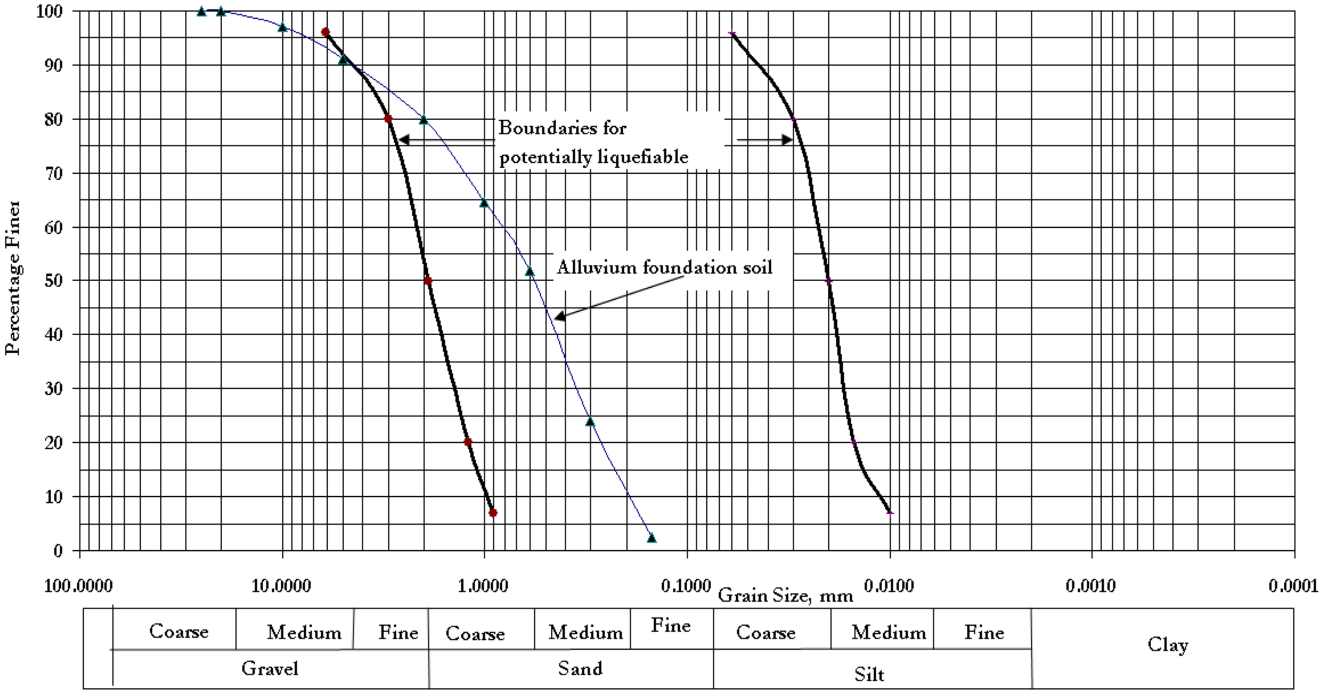

Fig. 2. Evaluation of liquefaction susceptibility of alluvium foundation using gradation curve (Tsuchida, 1970).

This paper presents a numerical study that investigates the influence of the canyon geometry and effect of ground conditions on the seismic performance of an earthfill dam. From the different seismic analysis results that are obtained from the different 3D simulations, the results are compared and correlated. From the results of the analyses and correlations created, the canyon geometry under which three dimensional behavior is of importance in the dynamic response of a dam are determined. And the resulting correlation is then applied to the seismic performance of the Tendaho earthfill dam. The results of the analysis give a clue which model (2D or 3D) to use for the problem at hand.

In this study, the analysis is conducted using a 3D finite difference modeling. The analyses are carried out within the framework of plasticity.

In order to investigate the effect of the canyon geometry on the seismic performance of earth dams, different valley configuration are considered. A typical 3D dam model is shown in Fig. 3.

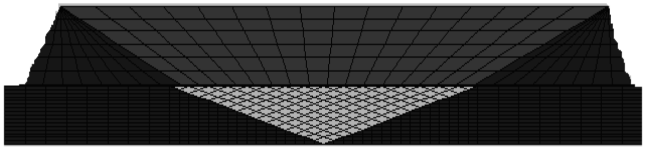

Fig. 3. Typical 3D model of dam along with the valley.

CONSTITUTIVE MODEL

The seismic concern of an earthfill dam is the development of large displacement that could endanger the safety and serviceability of the dam. Such movements depend on the earthquake loading, the geometry of the dam, and the strength properties of the materials of the dam and foundation, valley geometry and the ground water conditions. For the calculation of these movements, a 3D finite difference modeling FLAC3D is used during the dynamic analyses. The behaviors of the geomaterials are described by an elastic-plastic Mohr-Coulomb constitutive model. This is so because the elastoplastic analysis constitutes an efficient tool for the investigation of stability of dams under seismic loading. The seismically induced settlement could be used for the evaluation of the stability of the dam.

NUMERICAL MODEL

The numerical analyses are conducted using the finite difference program FLAC3D. This program is based on a continuum finite difference discretization using the Langrangian approach (FLAC3D, 2005). In this numerical model, the equations of motion are derived for a continuum media. And the equations of motion are used to obtain the velocities and displacements from stresses and forces. The strain rates are then calculated according to the new nodal velocities in each element.

To analyze the problem, the strain-rate tensor and rotation rate tensor can be written as follows:

$$\xi_{ij} = \frac{1}{2}\left(v_{i,j} + v_{j,i}\right) \tag{1}$$

$$\omega_{ij} = \frac{1}{2}\left(v_{i,j} - v_{j,i}\right) \tag{2}$$

where v_i is the deformation velocity and $v_{i,j}$ is the velocity gradient. The equation of motion is written as:

$$\sigma_{ij,j} + \rho b_i = \rho \frac{dv_i}{dt} \tag{3}$$

The constitutive equation can be written out in general as:

$$\Delta\breve{\sigma}_{ij} + \alpha \Delta p \delta_{ij} = H^{*}_{ij}(\sigma_{ij}, \Delta\varepsilon_{ij}) \tag{4}$$

$$\Delta\breve{\sigma}_{ij} + \alpha \Delta p \delta_{ij} = H^{*}_{ij}(\sigma_{ij}, \Delta\varepsilon_{ij}) \tag{5}$$

$$\breve{\sigma}_{ij} = H_{ij}\left(\sigma_{ij}, \xi_{ij}, \kappa\right) \tag{6}$$

where $\breve{\sigma}_{ij}$ is the co-rotational stress-rate tensor, H_{ij} is the constitutive function, and κ is a parameter, which takes into account the loading history. The co-rotational stress rate tensor is defined as follows

$$\breve{\sigma}_{ij} = \frac{d\sigma_{ij}}{dt} - \omega_{ik}\sigma_{kj} + \sigma_{ik}\omega_{kj} \tag{7}$$

$\frac{d\sigma_{ij}}{dt}$ is the material time derivative of σ.

The above equations are solved by finite difference method. A coupled calculation with dynamic groundwater flow is performed to determine the excess pore pressure. Regarding the mechanism of pore pressure generation, an empirical equation that relates the increment of volume decrease, $\Delta\varepsilon_{vd}$ to the cyclic shear-strain amplitude, γ, and accumulated irreversible volume strain , ε_{vd} is used (Byrne 1991)

$$\frac{\Delta\varepsilon_{vd}}{\gamma} = C_1 \exp\left(-C_2\left(\frac{\varepsilon_{vd}}{\gamma}\right)\right) \tag{8}$$

where C_1 and C_2 are material parameters, which vary according to the sand type. These parameters are estimated from the following relationships

$$C_1 = 7600\left(D_r\right)^{-2.5} \tag{9}$$

$$D_r = 15\sqrt{(N_1)_{60}} \tag{10}$$

$$C_2 = 0.4 / C_1 \tag{11}$$

where D_r and $(N_1)_{60}$ are the relative density and SPT blow counts corrected for energy respectively.

The dynamic loading is applied at the base of the foundation layer as an acceleration time history. The frequency content of the input motion and the velocity of the propagating waves affect the accuracy of the numerical solutions. For appropriate wave propagation through an element, the maximum element size, $\Delta x_{\max}$ has to be smaller than one-tenth to one-eighth of the wave length, λ. This wave length corresponds to the highest frequency component, f, that contains appreciable energy of the input motion. This is according to the recommendation by Kuhlemeyer and Lysmer (1973). Therefore $\Delta x_{\max} \le \lambda / 10$ is used in this study. From the seismic record analysis, the highest angular frequency of the input motion is about 15 rad/sec. Accordingly, the grid size or element size for the different materials of the dam body and the foundation are determined as shown in Fig. 3.

The Free-Field Boundaries are used to absorb the outward waves originating from the structure. This system of boundary condition involves the execution of free-field calculations in parallel with the main-grid analysis. The lateral boundaries of the main grid are coupled to the free-field grid by viscous dashpots to simulate a quiet boundary.

The Sigmoidal hysteretic damping with four parameters is used in the analyses for the energy dissipation through the medium.

DAM GEOMETRY AND MATERIAL PARAMETERS

The basic general geometry, zones and slopes of the earthfill dam considered are shown in Fig. 4. It consists of the following zones.

Zone 1: Impervious core (clay blended with sandy gravel).
Zones 2A & 2B: Shell (sandy gravel).
Zone 3: Transition zone (fine sand)
Zone 4: Filter Zone (coarse sand). And the soil properties of each zone are given in Table 1.

The dynamic properties used in this work are taken from Seed et al. (1986). Except the lake deposit, the maximum shear modulus of all materials is considered to vary with the mean effective stress according to the formula: $G_{\max} = 218.7 K_{2\max} \left(\sigma_m^{'}\right)^{0.5}$, where as for the lake deposit $G_{\max}=\rho(V_s)^2$ with the shear wave velocity V_s=1 km/sec. The values used for the coefficient $K_{2\max}$ are listed in Table 2 along with other soil parameter. The materials that are assumed to liquefy are modeled with the porewater pressure generation model proposed by Finn. The other materials are modeled with the Mohr-Coulomb constitutive model. The shear strength envelope is specified by friction angle and cohesion. The model parameters for the different materials of the dam body as well as the foundation are given in Table 1 and 2.

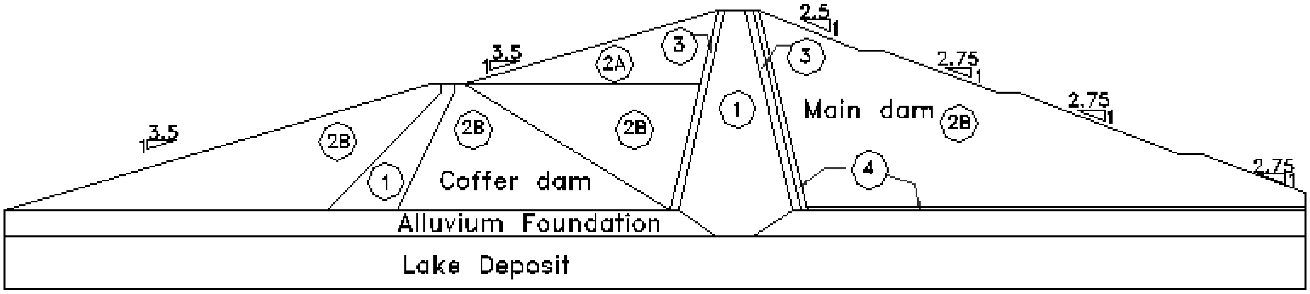

Fig. 4. Dam geometry and its zone (not to scale).

TABLE 1. ZONE MATERIAL PROPERTY

Property	**Zone**				
	1	2A	2B	3	4
Specific gravity, G_s	2.72	2.70	2.70	2.70	2.70
Dry density, (kg/m^3)	1600	1800	1800	1800	1800
Porosity, n	0.41	0.33	0.33	0.33	0.33
Permeability, k (m/s)	2.5×10^{-8}	5×10^{-5}	1×10^{-6}	1×10^{-5}	1×10^{-4}
Cohesion, c' (Pa)	7000	0	0	0	0
Friction angle, $\phi^{'}$ (^{o})	25	34	34	34	34

TABLE 2. MATERIAL PROPERTY.

Material	Poisson's ratio, ν	K_{2max}
Mixed clay core	0.34	40
Sandy gravel shell	0.3	90
Alluvium foundation	0.3	70

SEISMIC LOADING

As there is no acceleration time history in / or around the area, the commonly used acceleration time history for earthquake resistant design, the 1940 El Centro (California) earthquake is used, Fig. 5. The base line correction and filtering of the raw acceleration record is carried out. So this modified and scaled to different magnitudes is applied to the considered earthfill dam model.

DYNAMIC ANALYSIS RESULTS

The numerical model outlined above has been applied to four different cases of canyon geometry. The dynamic analysis is carried out for the horizontal El Centro earthquake scaled to different acceleration magnitudes, 0.15g, 0.3g and 0.6g.
The crest settlement time histories for the different slope considered are plotted in Fig. 6. The parameter m is the tangent of the slope angle of the valley from the horizontal. Moreover, just for the sake of illustration, crest settlement contours for three slope angles (20^0, 37^0 and 45_0) are plotted in Fig. 7, 8 and 9. In addition, the maximum crest settlements for different canyon geometries and different magnitude of earthquake acceleration are presented in Fig. 10.

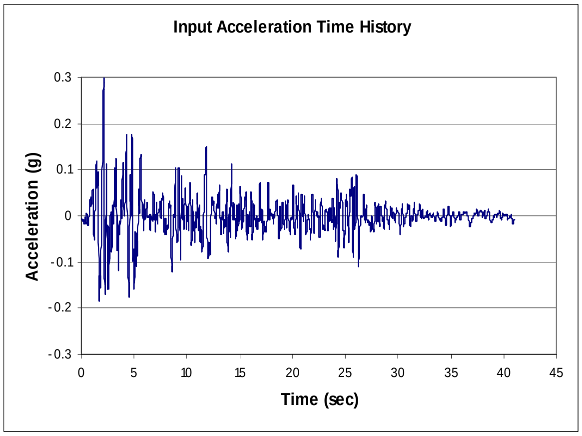

Fig. 5. Modified input acceleration time history.

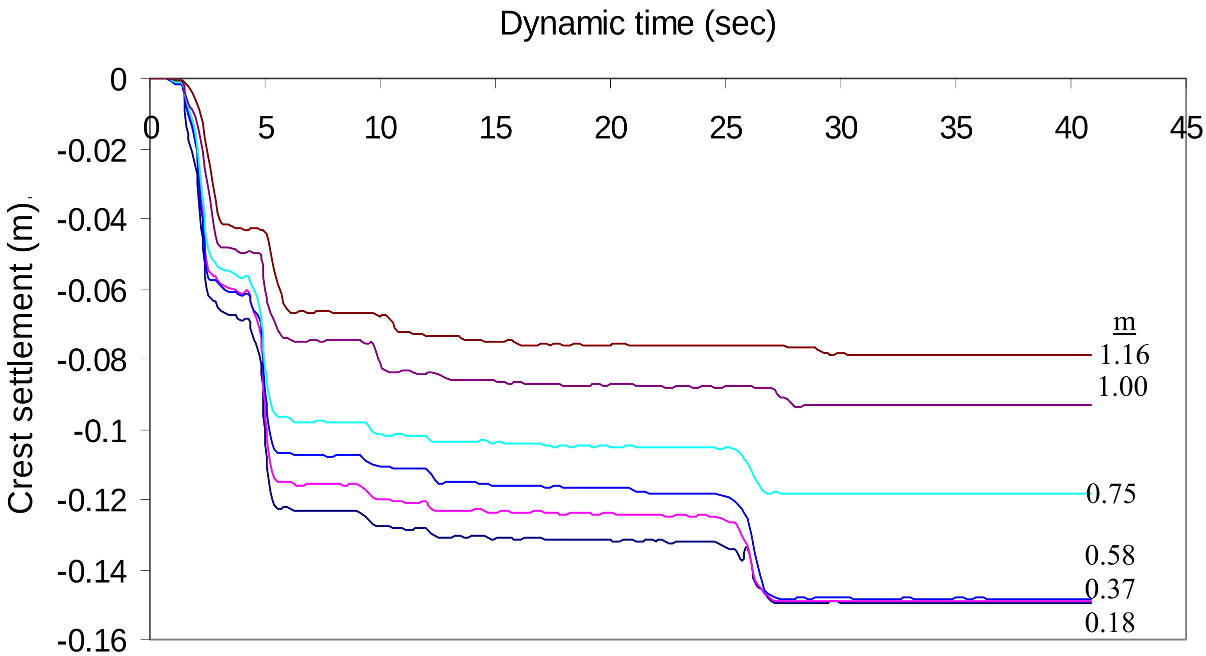

Fig. 6. Crest settlement versus dynamic time for different slope of valley (0.3g).

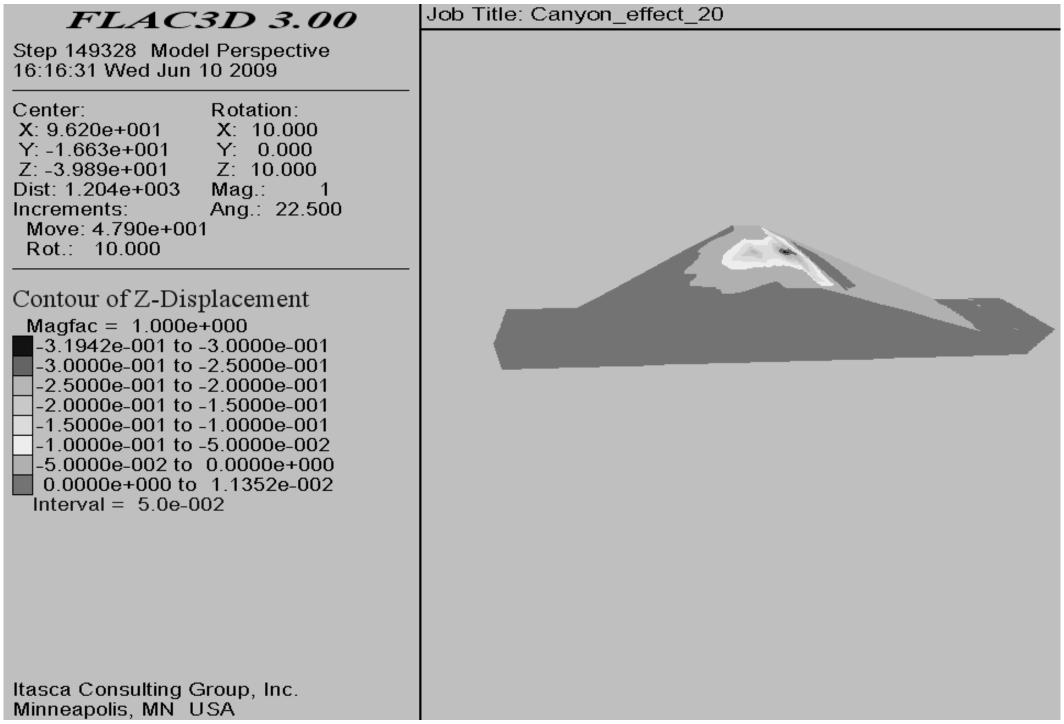

```
FLAC3D 3.00
Step 149328  Model Perspective
16:16:31 Wed Jun 10 2009

Center:                 Rotation:
 X: 9.620e+001           X:  10.000
 Y: -1.663e+001          Y:   0.000
 Z: -3.989e+001          Z:  10.000
Dist: 1.204e+003        Mag.:      1
Increments:             Ang.:  22.500
  Move: 4.790e+001
  Rot.:   10.000

Contour of Z-Displacement
  Magfac =  1.000e+000
 -3.1942e-001 to -3.0000e-001
 -3.0000e-001 to -2.5000e-001
 -2.5000e-001 to -2.0000e-001
 -2.0000e-001 to -1.5000e-001
 -1.5000e-001 to -1.0000e-001
 -1.0000e-001 to -5.0000e-002
 -5.0000e-002 to  0.0000e+000
  0.0000e+000 to  1.1352e-002
   Interval =  5.0e-002

Itasca Consulting Group, Inc.
Minneapolis, MN  USA

Job Title: Canyon_effect_20
```

Fig. 7. Crest settlement contours for angle of slope of 20^0.

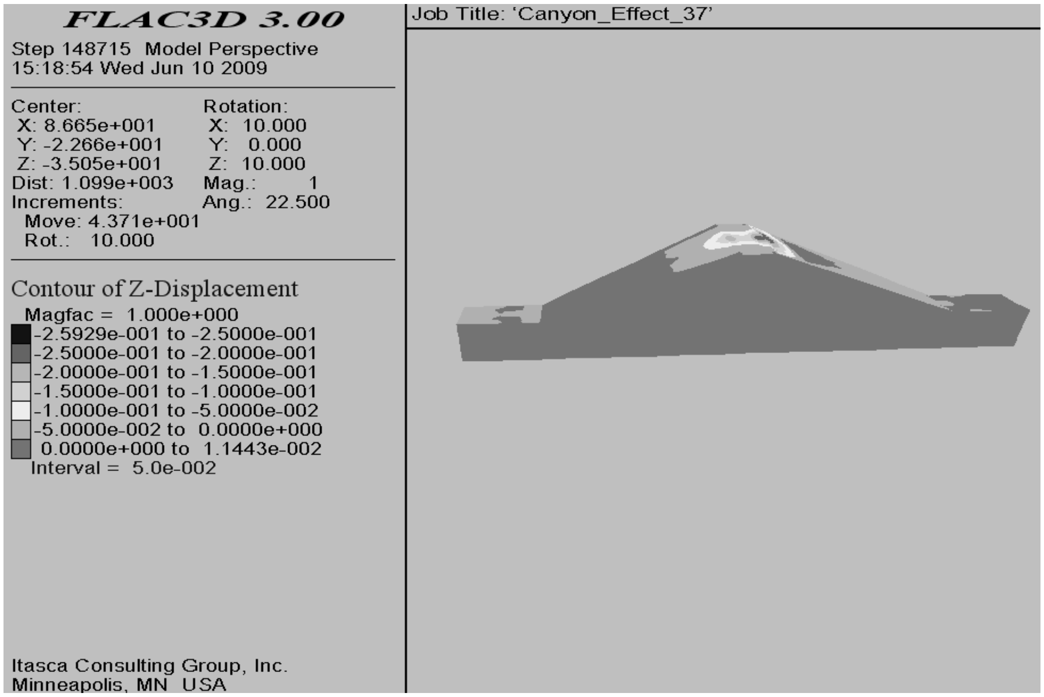

```
FLAC3D 3.00
Step 148715  Model Perspective
15:18:54 Wed Jun 10 2009

Center:                 Rotation:
 X: 8.665e+001           X:  10.000
 Y: -2.266e+001          Y:   0.000
 Z: -3.505e+001          Z:  10.000
Dist: 1.099e+003        Mag.:      1
Increments:             Ang.:  22.500
  Move: 4.371e+001
  Rot.:   10.000

Contour of Z-Displacement
  Magfac =  1.000e+000
 -2.5929e-001 to -2.5000e-001
 -2.5000e-001 to -2.0000e-001
 -2.0000e-001 to -1.5000e-001
 -1.5000e-001 to -1.0000e-001
 -1.0000e-001 to -5.0000e-002
 -5.0000e-002 to  0.0000e+000
  0.0000e+000 to  1.1443e-002
   Interval =  5.0e-002

Itasca Consulting Group, Inc.
Minneapolis, MN  USA

Job Title: 'Canyon_Effect_37'
```

Fig. 8. Crest settlement contours for angle of slope of 37^0.

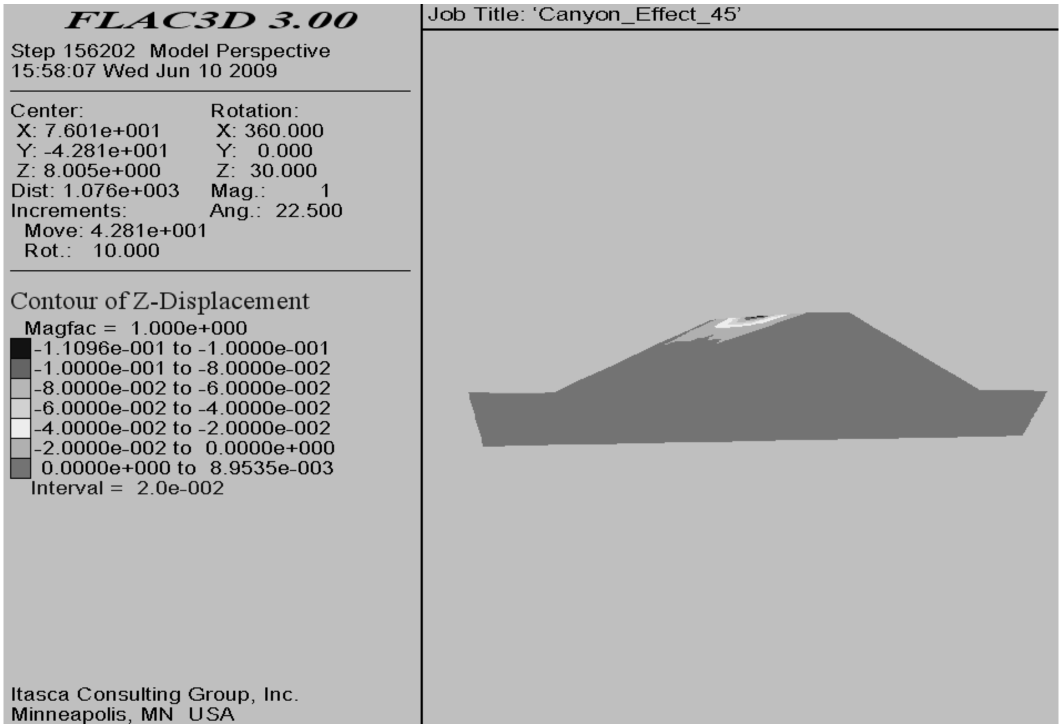
FLAC3D 3.00

Step 156202 Model Perspective
15:58:07 Wed Jun 10 2009

Center:
X: 7.601e+001
Y: -4.281e+001
Z: 8.005e+000
Dist: 1.076e+003
Increments:
Move: 4.281e+001
Rot.: 10.000

Rotation:
X: 360.000
Y: 0.000
Z: 30.000
Mag.: 1
Ang.: 22.500

Contour of Z-Displacement
Magfac = 1.000e+000
■ -1.1096e-001 to -1.0000e-001
■ -1.0000e-001 to -8.0000e-002
■ -8.0000e-002 to -6.0000e-002
■ -6.0000e-002 to -4.0000e-002
■ -4.0000e-002 to -2.0000e-002
■ -2.0000e-002 to 0.0000e+000
■ 0.0000e+000 to 8.9535e-003
Interval = 2.0e-002

Itasca Consulting Group, Inc.
Minneapolis, MN USA

Job Title: 'Canyon_Effect_45'

Fig. 9. Crest settlement contours for angle of slope of 45^0.

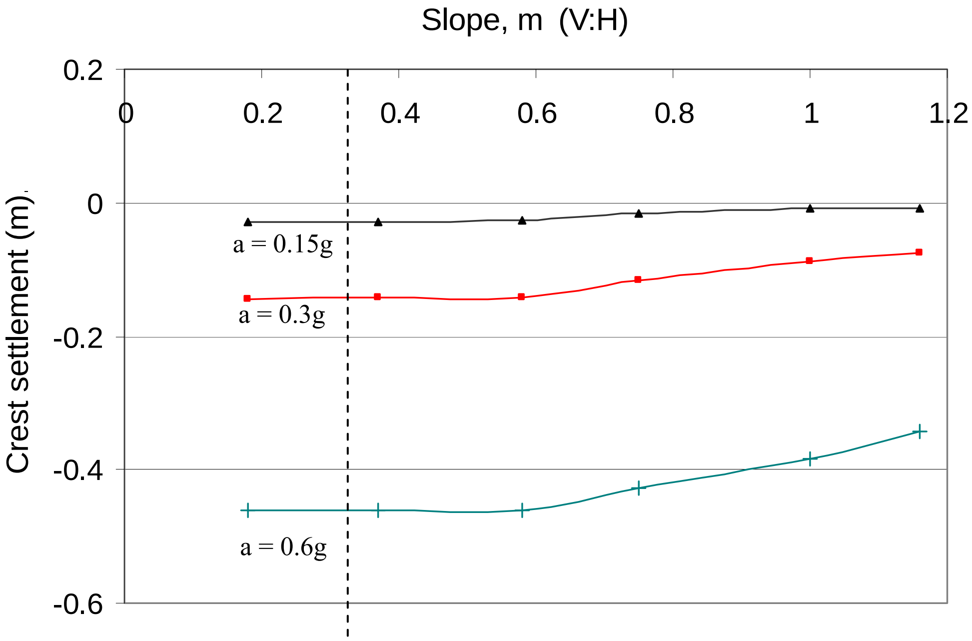

Fig. 10. Crest settlement versus slope of valley, m for different magnitude of accelerations.

The results of the analysis show that the canyon effect is highly pronounced for dams with tangent of slope angle of valley greater than about 0.5. An *m* value of 0.5 is equivalent to a slope angle of about 27^0. This effect decreases with decrease in the magnitude of the acceleration. The canyon effect diminishes with decrease in the value of the slope angle below about 27^0.

Relatively accurate crest settlement that takes into account the canyon shape can be estimated from the settlement value computed with the assumption of plane strain problem by employing the correction factor chart shown in Fig. 11. The correction factor, *cf*, is a function of the magnitude of the peak acceleration.

$$\Delta z = -cf\left(m - 0.5\right) \tag{12}$$

where;

Δz is correction value as function of the magnitude of the acceleration and the shape of the canyon.

cf is correction factor as a function of magnitude of acceleration.

m is tangent of slope angle of valley or canyon and has to be greater than 0.5 which is equivalent to 27^{o}. This is because corrections are required for slope angles greater than about 27^{0}.

The corrected crest settlement, z_c will then be given as:

$$z_c = \Delta z + z \tag{13}$$

where;

z is the crest settlement computed assuming plane strain problem.

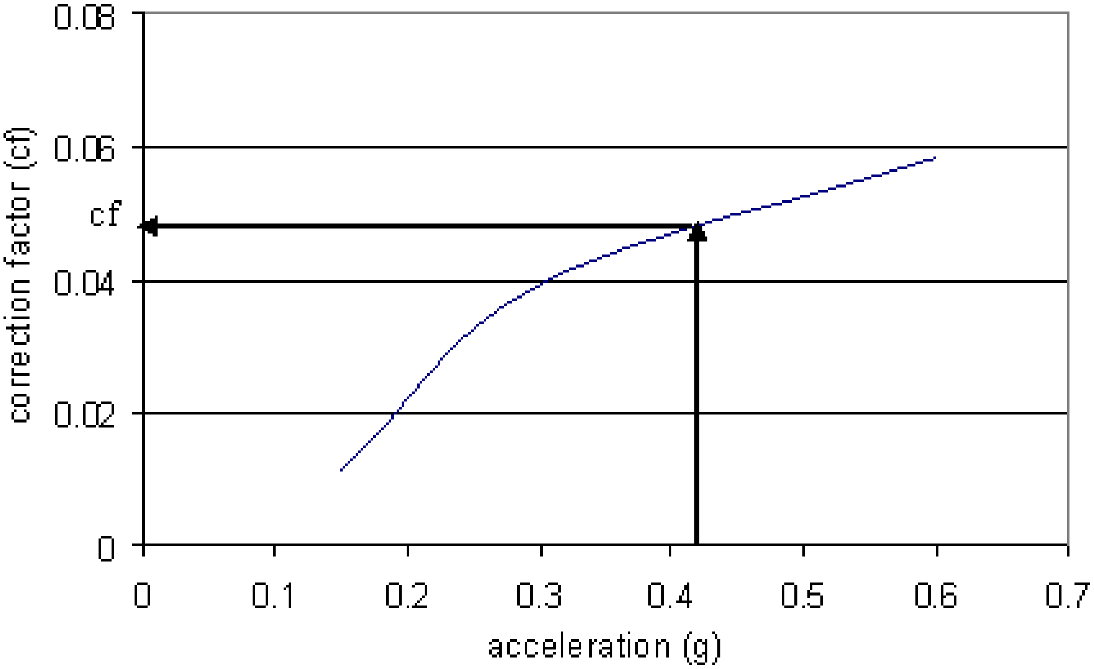

Fig. 11. Approximate correction factor (cf) versus magnitude of acceleration.

In addition to the canyon effect of the dam, the danger of liquefaction of the alluvium foundation material of the dam was evaluated. Based on the preliminary evaluation of liquefaction susceptible of the alluvium material, there is a danger of liquefaction. In addition the shell materials are assumed to liquefy. So in the dynamic analysis of the dam, the alluvium and shell material are assumed to liquefy and the analysis is carried out for two different peak ground acceleration, PGA magnitudes, the Maximum Credible Earthquake, MCE, and Operating Base Earthquake, OBE.

For the case considered, a maximum crest settlement of 0.80 m and maximum horizontal crest displacement of 2.11 m has been predicted under the action of MCE, Fig. 13. The same case was analyzed for the OBE, and a maximum crest settlement of 0.63 m is predicted.

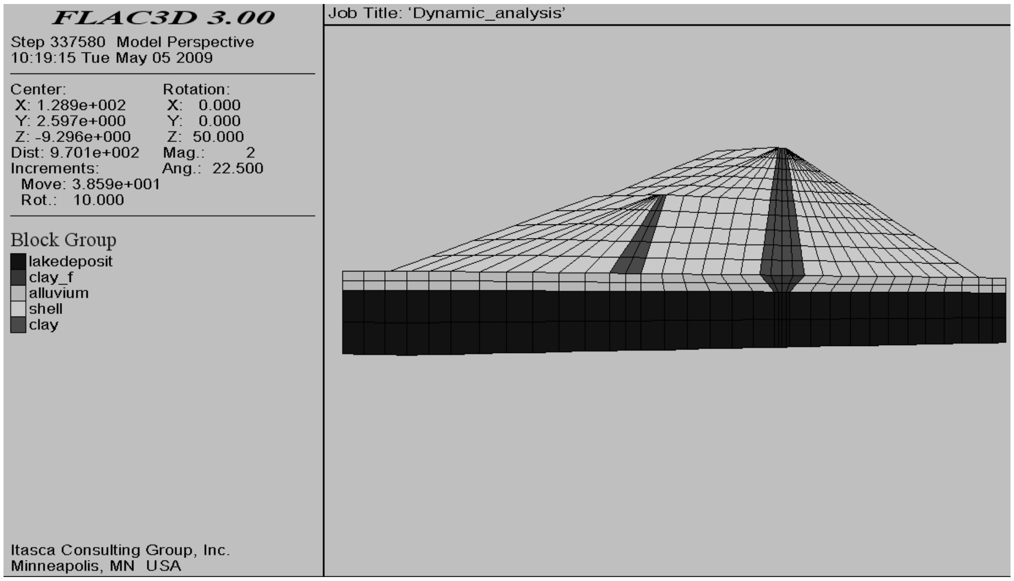

FLAC3D 3.00

Step 337580 Model Perspective
10:19:15 Tue May 05 2009

Center:
X: 1.289e+002
Y: 2.597e+000
Z: -9.296e+000
Dist: 9.701e+002

Rotation:
X: 0.000
Y: 0.000
Z: 50.000
Mag.: 2
Ang.: 22.500

Increments:
Move: 3.859e+001
Rot.: 10.000

Block Group
■ lakedeposit
■ clay_f
■ alluvium
■ shell
■ clay

Itasca Consulting Group, Inc.
Minneapolis, MN USA

Job Title: 'Dynamic_analysis'

Fig. 12. FLAC3D model of Tendaho earthfill dam.

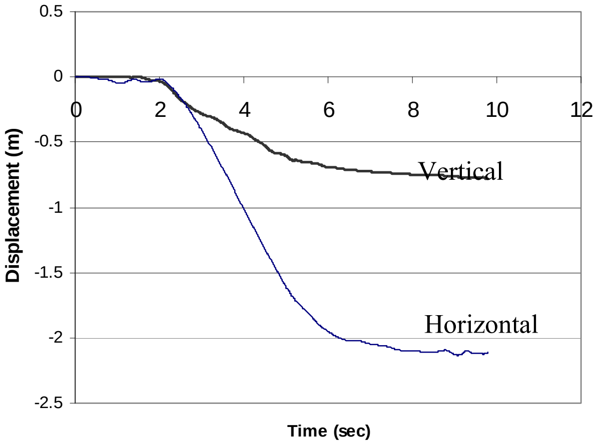

Fig. 13. Time history of horizontal and vertical displacement at the dam crest.

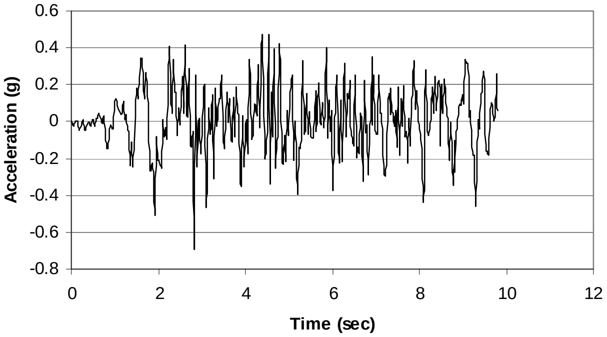

Fig. 14. Time history of acceleration response at the crest level.

The contours of pore water pressure as a result of the shaking for the MCE are shown in Fig. 15. From this figure it can be seen that the pore water pressure in the alluvium soil layer has reached 825 kPa from a neutral pore water pressure of 520 kPa. This gives an excess pore water pressure of about 305 kPa. This is near to the effective vertical stress (350 kPa) at the same point, see Fig. 17. In other words the pore pressure ratio is approaching 1 indicating an impending of liquefaction. As the phreatic line is lower in the downstream shell, the development of the pore pressure is limited. Consequently there is minimal movement of the downstream slope. Further computations after 10 seconds was not possible because of the excessive mesh distortion. This is the case for the MCE.

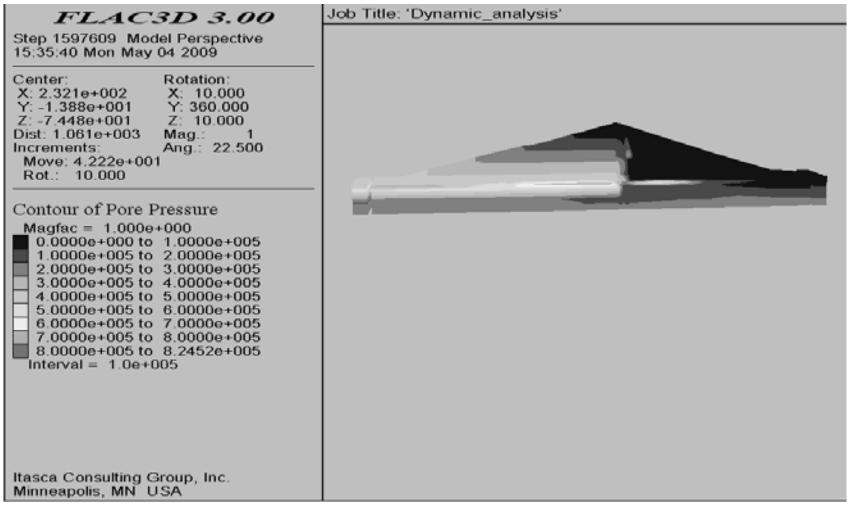

```
FLAC3D 3.00
Step 1597609  Model Perspective
15:35:40 Mon May 04 2009

Center:                Rotation:
 X: 2.321e+002          X:  10.000
 Y: -1.388e+001         Y: 360.000
 Z: -7.448e+001         Z:  10.000
Dist: 1.061e+003       Mag.:     1
Increments:            Ang.:  22.500
 Move: 4.222e+001
 Rot.:  10.000

Contour of Pore Pressure
 Magfac =  1.000e+000
■ 0.0000e+000 to  1.0000e+005
■ 1.0000e+005 to  2.0000e+005
■ 2.0000e+005 to  3.0000e+005
■ 3.0000e+005 to  4.0000e+005
■ 4.0000e+005 to  5.0000e+005
■ 5.0000e+005 to  6.0000e+005
■ 6.0000e+005 to  7.0000e+005
■ 7.0000e+005 to  8.0000e+005
■ 8.0000e+005 to  8.2452e+005
  Interval =  1.0e+005

Itasca Consulting Group, Inc.
Minneapolis, MN  USA

Job Title: 'Dynamic_analysis'
```

Fig. 15. Contour of pore water pressure for the MCE.

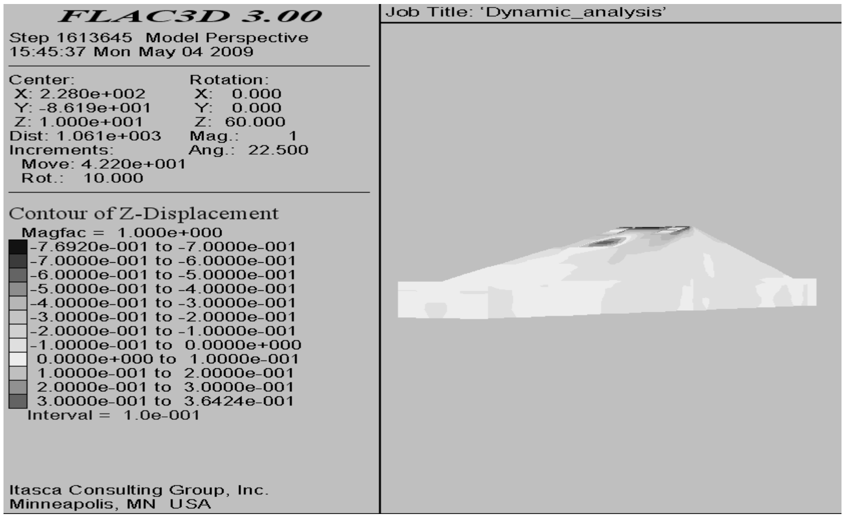

```
FLAC3D 3.00
Step 1613645  Model Perspective
15:45:37 Mon May 04 2009

Center:                Rotation:
 X: 2.280e+002          X:   0.000
 Y: -8.619e+001         Y:   0.000
 Z: 1.000e+001          Z:  60.000
Dist: 1.061e+003       Mag.:        1
Increments:            Ang.:  22.500
 Move: 4.220e+001
 Rot.:   10.000

Contour of Z-Displacement
 Magfac =  1.000e+000
■ -7.6920e-001 to -7.0000e-001
■ -7.0000e-001 to -6.0000e-001
■ -6.0000e-001 to -5.0000e-001
■ -5.0000e-001 to -4.0000e-001
■ -4.0000e-001 to -3.0000e-001
■ -3.0000e-001 to -2.0000e-001
■ -2.0000e-001 to -1.0000e-001
■ -1.0000e-001 to  0.0000e+000
■  0.0000e+000 to  1.0000e-001
■  1.0000e-001 to  2.0000e-001
■  2.0000e-001 to  3.0000e-001
■  3.0000e-001 to  3.6424e-001
  Interval =  1.0e-001

Itasca Consulting Group, Inc.
Minneapolis, MN  USA

Job Title: 'Dynamic_analysis'
```

Fig. 16. Deformation patterns of the dam for the MCE.

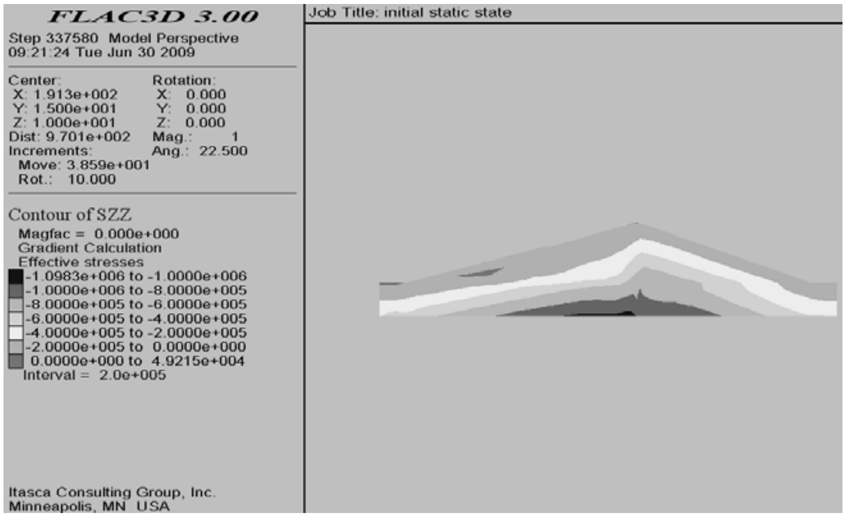

```
FLAC3D 3.00
Step 337580  Model Perspective
09:21:24 Tue Jun 30 2009

Center:                Rotation:
 X: 1.913e+002          X:  0.000
 Y: 1.500e+001          Y:  0.000
 Z: 1.000e+001          Z:  0.000
Dist: 9.701e+002       Mag.:      1
Increments:            Ang.:  22.500
 Move: 3.859e+001
 Rot.:  10.000

Contour of SZZ
 Magfac =  0.000e+000
 Gradient Calculation
 Effective stresses
■ -1.0983e+006 to -1.0000e+006
■ -1.0000e+006 to -8.0000e+005
■ -8.0000e+005 to -6.0000e+005
■ -6.0000e+005 to -4.0000e+005
■ -4.0000e+005 to -2.0000e+005
■ -2.0000e+005 to  0.0000e+000
■  0.0000e+000 to  4.9215e+004
  Interval =  2.0e+005

Itasca Consulting Group, Inc.
Minneapolis, MN  USA

Job Title: initial static state
```

Fig. 17. Contour of initial effective vertical stress.

CONCLUSIONS

From the results of analyses for the different shapes of the valley, the following important conclusions are drawn:

1. The canyon effect diminishes with decrease in the slope of the valley below about 27^0, two dimensional analyses can suffice for dams with are constructed on valley with slope less than about 27^0. But if the slope angle is greater than about 27^0, 3D analysis has to be carried out.
2. Plane strain analysis (2D) gives conservative results as compared to real 3D analysis. If plane strain analysis (2D) is carried out for dam to be constructed in valley with slope angle greater than about 27^0, then the analysis will be on the safe side. In the case where carrying out 3D model analysis is expensive then a 2D model analysis with reduction factor that takes the arching or canyon effect into account can be done.
3. It is found that the peak acceleration has a significant effect on the crest settlement. This effect decreases with decrease in the magnitude of the acceleration.
4. As far as the Tendaho dam is concerned, the angle of the slope varies from about 26^0 to 30^0 with the vertical which corresponds to m values of 0.49 and 0.58 respectively. The average value 0.54 is approximately equal to the demarcating value of m. For this reason, no correction value would be required, if plane strain analysis is executed.
5. The results of the FLAC dynamic analysis carried out using hysteretic damping indicate that displacements are concentrated near the crest of the dam.
6. The peak ground accelerations are predicted to be amplified from 0.3g at the base of the model to about 0.7g at the crest for the Tendaho dam. This corresponds to an amplification value of about 2.4.
7. A peak horizontal crest displacement of magnitude 1.88 m and peak crest settlements of 0.72 m are predicted. However, further increased value of crest displacement is possible because of the excessive liquefaction of the alluvium foundation soil and prolonged duration of the earthquake.

REFERENCES

Bawson, E. M. et al., [2001]. “A practical oriented pore-pressure generation model.” In: Billaux et al. (eds), Proc. of the 2nd Int. FLAC Symposium Lyon, France, Balkema, Rotterdam, pp. 47-54.

Bull, J.W., [1994]. “Soil-structure Interaction Numerical Analysis and Modeling.” First edition: E & FN Spon, UK.

Fang, H.Y., [2002]. “Foundation Engineering Handbook.” Kluwer Academic Publishers, USA, ISBN 0-412-98891-7.

Finn, W.D.L, [1979]. “Soil-dynamics-liquefaction of sands.” In: Proc. Int. Conf. Microzonation Vol. I, pp. 87–111 Seattle, Washington.

Gazetas, G. [1991]. “Foundation Vibrations”, in *Foundation Engineering Handbook*, (H.Y. Fang, ed.) Van Nostrand Reinhold, New York, NY, pp. 553-593.

Gopal Madabhushi, S. P., [2004]. “Modelling of earthquake damage using geotechnical centrifuges”, *Special section on Geotechnics and Earthquake hazards* Vol., 87, No. 10.

Itasca Consulting Group, Inc., [2005]. “FLAC3D - Fast Lagrangian Analysis of Continua in 3 Dimensions.” Version 3.0. Minneapolis, Minnesota, MN 55401.

John Krahn, [2004]. “Dynamic Modeling with QUAKE/W.” An Engineering Methodology, 1st edition, Geoslope international ltd, Canada.

Kenji Ishihara, [1996]. “Soil behaviour in earthquake geotechnics.” Clarendon Press, Oxford.

Prakash, S., Y. Wu and E.A. Rafnsson [1995a], “On Seismic Design Displacements of Rigid Retaining Walls”, *Proc. Third Intern. Conf. on Recent Adv. in Geo. Erthq. Engrg. and Soil Dyn.*, St. Louis, MO, Vol., III, pp. 1183-1192.

Parish, Y., Sadek, M., and Shahrour, I., [2009]. “Numerical analysis of the seismic behaviour of earth dam.” Natural Hazards Earth System Science, 9, pp. 451–458.

Robert, W. D., [2002]. “Geotechnical Earthquake Engineering Handbook.” The McGraw-Hill Companies, Inc, USA.

For additional information or clarification, please contact:
Mr. Tensay G. Berhe
Researcher
Institute of Geotechnical Engineering, BOKU
Vienna, A-1180, Feistmantel 4, Austria
Phone: +43 1 476564 5551
FAX: +43 1 476564 5567
E-mail: tensay@engineer.com